INEEL/CON-03-01199
PREPRINT

Extensions To SCDAP/RELAP5/ATHENA For Analysis Of HTGRS

Edwin A. Harvego
Larry J. Siefken

April 25 – 29, 2004

ICONE 12

Proceedings of ICONE 12
12th International Conference on Nuclear Engineering
April 25-29, 2004, Arlington, Virginia, USA

ICONE-12-49304

EXTENSIONS TO SCDAP/RELAP5/ATHENA FOR ANALYSIS OF HTGRS

Edwin A. Harvego/Idaho National Engineering and Environmental Laboratory/P. O. Box 1625/Idaho Falls, Idaho 83415/Phone: (208) 526-9544/Fax: (208) 526-2930/e-mail: hae@inel.gov

Larry J. Siefken/Idaho National Engineering and Environmental Laboratory/P. O. Box 1625/Idaho Falls, Idaho 83415/Phone: (208) 526-9319/Fax: (208) 526-2930/e-mail: ljs@inel.gov

ABSTRACT

The SCDAP/RELAP5/ATHENA code was extended to enable the code to perform transient analyses of two leading candidates for the next generation of nuclear power plants, namely the Pebble Bed and Block-Type (prismatic) High Temperature Gas Reactors (PB-HTGRs and BT-HTGRs). Models in five areas of reactor behavior were implemented into the code. First, models were implemented to calculate the transfer of decay heat by conduction and radiation from the center of the heterogeneous cores of these reactors to their outer surfaces. Second, models were implemented to calculate the transfer of decay heat from the outer surfaces of these reactor cores to ultimate heat sinks such as the atmosphere. Third, models were implemented to calculate the flow losses and convective heat transfer in the core of a PB-HTGR. Fourth, models were implemented to calculate the oxidation of graphite due to the ingress of air. Fifth, a model was implemented to calculate the ingress of air into the reactor core by molecular diffusion from the point of break in the coolant system. The extended code was applied to the analysis of conduction cooldown accident in a BT-HTGR. The analysis indicated that the new models in SCDAP/RELAP5/ATHENA are properly interfaced with the previously developed and assessed fluid behavior models in the code. Preliminary results indicate that post-shutdown decay heat can be adequately removed from BT-HTGRs by natural circulation of air from the atmosphere.

INTRODUCTION

Leading reactor designs for the future production of nuclear energy include the Pebble Bed High Temperature Gas Reactor (PB-HTGR) [1, 2, 3] and the Block Type (prismatic) High Temperature Reactor (BT-HTGR) [4, 5]. These reactors can have a direct Brayton thermodynamic cycle for very efficient conversion of nuclear power into electricity and exhibit relatively benign behavior under various accident conditions. The PB-HTGRs and BT-HTGRs use helium as the primary coolant and graphite as the material for moderating neutrons. The PB-HTGR reactor core is configured as a deep bed of spherical pebbles the size of billiard balls (diameter of approximately 60 mm). Each pebble has about 15,000 embedded small fuel particles (diameter of about 0.5 mm). The BT-HTGR reactor core is configured as blocks of graphite containing fuel compacts (fuel rods) and coolant channels. The fuel compacts are composed of graphite with fuel particles. For both the PB-HTGR and BT-HTGR, the fuel particles have a ceramic coating that retains fission products even during temperature escalations caused by a reactor accident. The fuel in these reactors can sustain a high level of burnup and thus promotes a reduction in radioactive waste. Also, the helium coolant does not become radioactive with irradiation and thus contributes further to a reduction in radioactive waste. After burnup, the fuel particles can be placed without processing in a wet or dry repository and remain resistant to corrosion for hundreds of thousands of years [6, 7]. The great difficulty in breaking down the coatings on spent fuel particles promotes proliferation resistance [7]. The reactors can be built as small as 100 MWe and thus can be built with a relatively small capital investment. The high thermal efficiency of the reactors also reduces cost and waste.

This paper describes the extension of the SCDAP/RELAP5-3D/ATHENA computer code for the transient analysis of these advanced reactor designs. This code has been widely assessed and used for the transient analysis complex configurations of fluid and heat transport systems. The addition of models for the peculiar phenomena in PB-

HTGRs and BT-HTGRs equips the code for the transient analysis of these advanced reactor designs.

1. MODELS FOR HEAT CONDUCTION THROUGH HETEROGENEOUS REACTOR CORE.

In the event of a large break in the primary system of a PB-HTGR or BT-HTGR, the long-term temperature distribution in the reactor core is the result of the transport of decay heat by conduction and radiation through the porous or heterogeneous medium of the reactor core to its exterior surface. The temperature distribution through the reactor core is calculated solving the two-dimensional (radial-axial) heat conduction equation using effective thermal conductivities to represent heat transfer by conduction and radiation in a porous or heterogeneous medium. The heterogeneous solid part of the reactor core and its gaseous parts are homogenized as a continuum with heat transfer characteristics representative of the actual heterogeneous configuration of the reactor core. Using the two-dimensional cylindrical coordinate system, the equation solved for the transient temperature distribution of the reactor core is the integral form of the heat conduction equation for an anisotropic continuum. This equation is [8]:

$$\int_v \rho c_p \frac{\partial T}{\partial t}\, dv = \int_v \frac{\partial}{r\partial r}\left(r k_r \frac{\partial T}{\partial r}\right) dv + \int_v \frac{\partial}{\partial z}\left(k_z \frac{\partial T}{\partial z}\right) dv$$

$$+ \int_v Q_v\, dv + \int_s Q_s\, ds \qquad (1\text{-}1)$$

where

Q_v = net volumetric heat generation (nuclear and oxidation heat generation and heat removal by convective cooling, W/m^3)

Q_s = heat flux at the boundaries of the continuum (convective, radiative, W/m^2)

T = temperature at location (r, z) at time t where r and z are the radial and axial coordinates, respectively (K)

ρc_p = volumetric heat capacitance ($J/m^3 \cdot K$)

k_r, k_z = effective thermal conductivity in the radial and axial directions, respectively (W/m·K).

Equation (1-1) is solved using the finite difference and finite volume methods [8, 9].

The effective thermal conductivity is calculated as a function of the temperature, composition, and configuration of the various elements in the reactor core. The calculated effective thermal conductivity accounts for several modes of heat transfer, including heat conduction through the solid parts of the core, heat conduction through gases in the interstices in a PB-HTGR core and through gases in the coolant channels and gaps in a BT-HTGR core, radiation heat transfer across interstices in a PB-HTGR core and across coolant channels and gaps in a BT-HTGR core, and heat conduction through points of contact of the pebbles in a PB-HTGR core. The effective thermal conductivity for the core of the PB-HTGR is calculated by the NO correlation [10] or the Tanaka and Chisaka correlation for a discontinuous solid system [11]. The effective thermal conductivity for the core of the BT-HTGR is calculated by the Tanaka and Chisaka correlation for a continuous solid system. The NO correlation is an empirically based correlation applicable only to a PB-HTGR core. The Tanaka and Chisaka correlations have application to a wide range of heterogeneous media.

The NO correlation for effective thermal conductivity [10] combines the conduction and radiation contributions to heat transfer into one simple empirical correlation. This correlation is applicable only for a bed of fuel pebbles similar to that from which data was obtained for establishing the correlation. This correlation is

$$k_r = k_z = 1.1536 \times 10^{-4}\ (T - 173.16)^{1.6632} \qquad (1\text{-}2)$$

where

$k_r = k_z$ = effective overall thermal conductivity in radial and axial directions (W/m·K),

T = temperature (K).

The Tanaka and Chisaka correlation for the case of a medium composed of continuous solid material is expressed by the equation

$$k = \left[A + (1 - A)\frac{\log[1 + 2B(k_{por}/k_s - 1)]}{2B(1 - k_s/k_{por})} \right] k_s$$

$$+ k_{rad} \qquad (1\text{-}3)$$

where

k = overall effective thermal conductivity of a heterogeneous medium (W/m·K),

A = $2(1 - \varepsilon)/(2 + \varepsilon)$

B = $(1 - \varepsilon)/3$

ε = porosity of the medium

k_s = thermal conductivity of the solid material in the porous medium (W/m·K)

k_{por} = thermal conductivity of the material or gas in the pores of the porous medium (W/m·K)

k_{rad} = contribution of radiation heat transfer to effective thermal conductivity (W/m·K).

In the above equation, the "A" term represents the parallel void ratio and the "B" term represents the series void ratio. For the case of the material in the pores of the medium being composed only of gas, the thermal conductivity of the pores is calculated by subroutine gascns in the Material Properties Package (MATPRO) in SCDAP/RELAP5/ATHENA [12]. The porosity of the reactor core of a PB-HTGR is calculated by the empirical equation [10]

$$\varepsilon = 0.375 + 0.78/(D_{bed}/D_p)^2 \qquad (1\text{-}4)$$

where

D_{bed} = diameter of pebble bed (m)

D_p = diameter of pebbles (m).

The above equation is appropriate for spherical pebbles that are randomly packed.

The lower bound on effective thermal conductivity is calculated by representing the solid elements in the medium as not being in significant contact with each other. The Tanaka and Chisaka correlation for this configuration is expressed by the equation

$$k = \left[A_2 + (1 - A_2)\frac{\log[1 + 2B_2(k_s/k_{por} - 1)]}{2B_2(1 - k_{por}/k_s)} \right] k_{por} + k_{rad} \qquad (1\text{-}5)$$

where

A_2 = $2\varepsilon/(3 - \varepsilon)$

B_2 = $\varepsilon/3$.

In applying the above equation to a PB-HTGR, the thermal conductivities in the radial and axial direction are

$k_r = k_z = k$.

The thermal conductivity of the solid material in the fuel region of a PB-HTGR is equal to the thermal conductivity of the fuel pebbles. A correlation for the thermal conductivity of the fuel pebbles is [13]

$$k_s = 127.68\left[\left(\frac{0.06829 - 0.3906x10^{-4}(T - 273.16)}{n_{fs} + 1.931x10^{-4}(T - 273.16)}\right)\right] + 127.68\left[1.228x10^{-4}(T - 273.16) + 0.0462\right] \qquad (1\text{-}6)$$

where

n_{fs} = fast neutron irradiation dose [(fast neutrons/m^2)/1x10^{21})].

For the PB-HTGR, the radiation contribution term is applied in the overall effective thermal conductivity for the Tanaka and Chisaka correlation. This radiation term is calculated by the equation

$$k_{rad} = 4e_m \varepsilon\sigma D_p T^3 \qquad (1\text{-}7)$$

where

e_m = emissivity of surface of the pebbles

σ = Stefan-Boltzmann constant (5.66840^{-8} W/m^2·K^4)

D_p = diameter of pebbles (m)

T = temperature of pebbles (K).

The code user may select either the NO correlation or the Tanaka and Chisaka correlation for a discontinuous solid system.

The effective thermal conductivities calculated by the two models were compared for a packed bed of fuel pebbles with a diameter of 50 mm, a bed porosity of 0.388 and the fuel pebbles at a temperature of 1200 K. The conductivities of the fuel pebbles and the gas in the interstices of the fuel pebbles were 42.8 W/m·K and 0.4009 W/m·K, respectively. The radiation contribution term in these correlations had a value of 6.08 W/m·K. This value of the radiation contribution was based on an emissivity of 0.8 for the surface of the fuel pebbles. The effective thermal conductivities as calculated by the continuous solid system and the discontinuous solid system versions of the Tanaka and Chisaka correlation were 19.1 W/m·K and 9.9 W/m·K, respectively. For the same conditions, the NO model calculated a thermal conductivity of 11.7 W/m·K. The thermal conductivities as calculated by the NO correlation and the Tanaka and Chisaka correlation for a discontinuous solid system are in fairly close agreement (11.7 W/m·K versus 9.9 W/m·K).

The overall effective thermal conductivity in the radial direction of fuel blocks in a BT-HTGR is calculated by applying in two stages the Tanaka and Chisaka correlation for continuous solid systems, and then applying a term to account for radial gaps between the blocks. Figure 1 shows an example of the configuration of fuel blocks. A schematic of this method of calculating the overall thermal conductivity of a homogenized fuel block is shown in Figure 2. In the first stage, the effective thermal conductivity of the part of the fuel blocks with graphite block material and fuel compacts is calculated. In this stage, the fuel compacts are the discontinuous part of the medium and the graphite block material is the continuous part of the medium. The thermal conductivity of the discontinuous part of the medium is the thermal conductivity of the fuel compacts and the thermal conductivity of the continuous part of

the medium is the thermal conductivity of the graphite block material. In the second stage, the effective thermal conductivity of the fuel block exclusive of the radial gaps between the fuel blocks is calculated. In this stage, the coolant channels are the discontinuous part of the system and the homogenized block material and fuel compacts are the continuous part of the system. The thermal conductivity of the gases in the coolant channel is calculated using a revised version of the gascns subroutine of the MATPRO database in SCDAP/RELAP5/ATHENA [12,14]. The thermal conductivity of the continuous part of the system for the second stage of calculations is calculated using the effective thermal conductivity calculated in the first stage of the calculations.

The presence of radial gaps between fuel blocks in a BT-HTGR is taken into account by applying an equation for effective thermal conductivity of a medium with radial gaps in it [15];

$$k_r = \frac{1}{\left(\frac{1}{h_{gap}\Delta r_{blk}}\right) + \frac{1}{k_{st2}}} \qquad (1\text{-}8)$$

where

k_r = overall effective thermal conductivity in radial direction of fuel blocks (W/m·K),

h_{gap} = conductance of radial gaps between blocks (W/m^2·K),

Δr_{blk} = width of fuel blocks in radial direction (m),

k_{st2} = effective thermal conductivity from second stage of calculations for effective thermal conductivity in radial direction of blocks (W/m·K).

The conductance of the radial gap between fuel and reflector blocks is calculated using the equation

$$h_{gap} = k_{gas} / t_{gap} \qquad (1\text{-}9)$$

where

k_{gas} = thermal conductivity of the gas in the gap (W/m·K),

t_{gap} = thickness of the gap in the radial direction (m).

The effective thermal conductivity in the axial direction of BT-HTGRs is calculated assuming no discontinuities in the axial direction. A multiplier is applied to account for the reduction in area due to the presence of coolant channels and fuel compacts. The thermal conductivity of the fuel compacts is assumed to be much smaller than that of the fuel blocks. Thus, the thermal conductivity in the axial direction is calculated by the equation

$$k_z = (1. - f_c)(1. - f_{cm})k_B \qquad (1\text{-}10)$$

where

k_z = effective thermal conductivity of fuel block in axial direction and with multiplier to account for reduction in area for heat conduction due to presence of coolant channels and fuel compacts (W/m·K),

f_c = ratio of area of coolant channels in fuel block to overall area of fuel block (horizontal plane),

f_{cm} = ratio of area of fuel compacts in fuel block to overall area of fuel block (horizontal plane),

k_B = thermal conductivity of graphite in fuel block (W/m·K).

The calculation of the volumetric heat source in the reactor core of a HTGR is calculated accounting for the fission and decay heat produced in the fuel, the heat produced by the oxidation of the graphite in the core and surrounding the reactor core, and the heat transferred to the coolant flowing through the reactor core. The transient and spatial distribution of fission and decay heat is calculated by the equation

$$q_{fd}(r,z) = G(t)\, F(r,z) \qquad (1\text{-}11)$$

where

$q_{fd}(r,z)$ = volumetric heat generation due to fission and decay heat at radial coordinate r and axial coordinate z of the reactor core (W/m^3),

G(t) = average volumetric heat generation in reactor core at time t due to fission and decay heat (W/m^3),

F(r,z) = ratio of volumetric heat generation at position (r,z) in the reactor core to average core volumetric heat generation rate.

The net volumetric heat generation is calculated by the equation

$$Q_v(r,z) = q_{fd}(r,z) + q_{ox}(r,z) - q_{cv}(r,z) \qquad (1\text{-}12)$$

where

$Q_v(r,z)$ = net volumetric heat generation in reactor core at position (r,z) (W/m^3),

$q_{ox}(r,z)$ = volumetric heat generation due to oxidation of graphite at position (r,z) (W/m^3),

$q_{cv}(r,z)$ = volumetric rate of removal of heat at position (r,z) due to convective heat transfer to coolant flowing through the reactor core (W/m^3).

For a conduction cooldown accident without air ingress, the last two terms on the right side of the above equation are negligible.

The volumetric heat capacity term in Equation (1-1) can be calculated by volume averaging of the various constituents in the reactor core. For PB-HTGRs, correlations are available for calculating the volumetric heat capacity of the reactor core [13].

The surface heat flux term in Equation (1-1) is a function of the convective and radiative heat transfer at the external surface of the reactor core. Models are used for convective heat transfer that account for forced flow and natural convection. These models are described elsewhere [16]. The model for radiative heat transfer is described in Section 2.

2. TRANSPORT OF DECAY HEAT TO ULTIMATE HEAT SINK.

HTGRs can be designed to transfer decay heat in a passive manner to heat sinks such as the atmosphere and the earth surrounding the reactor containment or building. This capability for passive cooling is in part due to the capability of a HTGR reactor core to endure temperatures as hot as 1900 K. Models are applied for calculating the transport of decay heat by conduction, radiation, and convection from the exterior surfaces of the reactor core to ultimate heat sinks such as the atmosphere and earth surrounding the reactor building. These models evaluate the capability of a reactor design to remove decay heat in a passive manner during accident such as the conduction cooldown accident. Structures in the path to the ultimate heat sink may include (1) reactor vessel, (2) upcomer, (3) downcomer, and (4) containment and surrounding earth. Decay heat is transported through these structures by conduction and between these structures by radiation and convection. Previously developed and assessed RELAP5 fluid transport models and convective heat transfer correlations calculate the convective heat transfer at the surfaces of these structures. A two-dimensional (radial-axial) heat conduction model calculates the heat transfer through these structures. The MATPRO material property package [12] calculates the thermal conductivities and volumetric heat capacities of the various materials in the reactor vessel, upcomer, downcomer, containment, and any surrounding earth. Boundary conditions are applied to the heat conduction model that correspond with the heat transfer occurring by radiation and convection at the surfaces of the various structures in the reactor system. Thus the transfer of heat is modeled through the entire media from the center of the reactor core to the ultimate heat sink such as the atmosphere and the earth surrounding the reactor containment or building.

A schematic of the modeling for the case of passive cooling to the atmosphere, containment, and surrounding earth is shown in Figure 3. In this case, downcomer and upcomer structures define the path for the natural circulation of air from the atmosphere. The horizontal cross section of the upcomer may have two configurations. In the first configuration, the air flows upward through an annular flow path. In the second configuration, the air flows upward through a series of individual structures arranged in a circle around the reactor vessel as shown in Figure 4. If the risers, downcomer, and containment have a square configuration instead of a circular configuration in a horizontal cross section, adjustments in the radii of these structures are made so the modeling approximates the overall heat transfer in the reactor system.

The models for convective heat transfer at the surfaces of the structures between the outer surface of the reactor core and the containment are calculated using conventional correlations [16]. The models for radiative heat transfer from the cylindrical shaped surfaces between the reactor core and containment are calculated using the conventional equations.

A new model was required to calculate heat transfer for the case of the upcomer consisting of a series of individual risers, as shown in Figure 4. In this case, the radial temperature distribution through the riser is calculated by representing the riser as a porous body. The boundary conditions applied to the riser are (1) radiative and convective heat fluxes on surface of riser facing the reactor vessel, (2) radiative and convective heat fluxes on side of riser facing the downcomer, and (3) convective heat transfer on internal surfaces of the riser.

The radiative heat transfer is calculated between three pairs of surfaces as shown in Figure 4. The radiative heat flux at the outer surface of the reactor vessel is calculated by the equation

$$q_{vo} = q_{vu1} + q_{vd1} \qquad (2\text{-}1)$$

where

q_{vo} = average radiative heat flux at outer surface of reactor vessel (W/m^2),

q_{vu1} = radiative heat flux at outer surface of reactor vessel due to radiation between outer surface of reactor vessel and inner surface of riser (W/m^2),

q_{vd1} = radiative heat flux at outer surface of reactor vessel due to radiation between outer surface of reactor vessel and inner surface of downcomer (W/m^2).

The variable q_{vu1} in Equation (2-1) is calculated by the equation

$$q_{vu1} = \left(\frac{w_u}{w_s}\right)\sigma \left(\frac{1.}{\frac{1.}{e_{vo}} + \left(\frac{R_{vo}}{R_{ui}}\right)\left(\frac{1.}{e_{ui}} - 1.\right)} \right)\left(T_{vo}^4 - T_{ui}^4\right) \quad (2\text{-}2)$$

where

w_u = width of individual riser (defined in Figure 4) (m),

w_s = spacing between individual riser (defined in Figure 4) (m),

T_{vo} = temperature of outer surface of reactor vessel (K),

T_{ui} = temperature of inner surface of riser (K),

e_{vo} = emissivity of outer surface of reactor vessel,

e_{ui} = emissivity of inner surface of riser.

R_{vo} = radius of outer surface of reactor vessel (m),

R_{ui} = radius of inner surface of riser (m).

The variable q_{vd1} is calculated by the equation

$$q_{vd1} = \left(\frac{w_s - w_u}{w_s}\right)\sigma \left(\frac{1.}{\frac{1.}{e_{vo}} + \left(\frac{R_{vo}}{R_{di}}\right)\left(\frac{1.}{e_{di}} - 1.\right)} \right)\left(T_{vo}^4 - T_{di}^4\right) \quad (2\text{-}3)$$

where

T_{di} = temperature of inner surface of downcomer (K),

R_{di} = radius of inner surface of downcomer (m),

e_{di} = emissivity of inner surface of downcomer.

The radiative heat flux at the inner surface of the riser is calculated by the equation

$$q_{ui} = \left(\frac{R_{vo}}{R_{ui}}\right) q_{vu1} \quad (2\text{-}4)$$

where

q_{ui} = radiative heat flux at inner surface of riser (W/m^2).

The radiation heat flux at the inner surface of the downcomer is calculated by the equation

$$q_{di} = q_{vd1} + q_{ud1} \quad (2\text{-}5)$$

where

q_{di} = average radiation heat flux on inside surface of downcomer (W/m^2),

q_{ud1} = heat flux on inner surface of downcomer due to radiation between outer surface of riser and inner surface of downcomer (W/m^2).

The radiative heat flux on the outer surface of the riser is calculated by the equation

$$q_{uo} = \left(\frac{w_u}{w_s}\right)\sigma \left(\frac{1.}{\frac{1.}{e_{uo}} + \left(\frac{R_{uo}}{R_{di}}\right)\left(\frac{1.}{e_{di}} - 1.\right)} \right)\left(T_{uo}^4 - T_{di}^4\right) \quad (2\text{-}6)$$

The variable q_{ud1} is calculated by the

$$q_{ud1} = \left(\frac{R_{uo}}{R_{di}}\right) q_{uo} \quad (2\text{-}7)$$

3. FLOW LOSSES

While the flow losses in BT-HTGRs are calculated with conventional flow loss correlations, a flow loss model based on Darcy's Law [17] was implemented to calculate the flow losses in PB-HTGRs. The flow losses are calculated in terms of drag force (pressure loss gradient). The flow losses are calculated as a function of several variables; (1) porosity of pebble bed, (2) diameter of pebbles, (3) viscosity and density of gas in interstices of pebbles, and (4) velocity of gas in interstices of pebbles. The flow losses are calculated by the equation [18]

$$F_p = \varepsilon\left[\frac{\mu j}{k} + \frac{\rho j^2}{m}\right] \quad (3\text{-}1)$$

where

F_p = flow resistance (N/m^3),

ε = porosity of the debris,

μ = viscosity of the gas (kg/m·s),

ρ = density of the gas (kg/m^3),

j = superficial velocity of the gas (m/s),

k = Darcy permeability of the pebble bed (m^2),

m = passability of the debris bed (m).

The second term on the right hand side of the above equation represents the turbulent drag counterpart to the viscous drag represented by the first term.

The Darcy permeability is calculated by the equation [18]

$$k = \frac{\varepsilon^3 D_p^2}{150(1-\varepsilon)^2} \quad (3\text{-}2)$$

where

D_p = diameter of pebbles (m).

The passability of the pebble bed is calculated by the equation [18]

$$m = \frac{\varepsilon^3 D_p}{1.75(1-\varepsilon)} \quad (3\text{-}3)$$

The flow losses are incorporated in the terms in the momentum field equation for losses due to friction and form. A condensed version of the field equation for momentum is

$$\rho\ \frac{\partial v}{\partial t} + \frac{1}{2}\rho\ \frac{\partial v^2}{\partial x} = -\frac{\partial p}{\partial x} + \cdots \quad (3\text{-}4)$$

where

ρ = density of gas (kg/m^3),

v = velocity of gas (m/s),

t = time (s),

x = spatial coordinate (m),

p = pressure of gas (N/m^2).

In the above equation, the first term on the left side of the equation is the acceleration of the gas, the second term on the left hand side is the momentum flux, and the first term on the right hand side is the pressure gradient.

The numerical solution scheme in SCDAP/RELAP5/ATHENA is based on replacing the differential equation form of the field equations with finite difference equations partially implicit in time. The difference equations are based on the concept of control volumes and a staggered spatial mesh. The pressures and energies are defined at volumes, and the velocities are defined at junctions. When the momentum equation is finite differenced (using integration over the momentum control volume centered on a junction), an additional variable named H_{loss} occurs on the right hand side of Equation (3-4). This variable accounts for losses due to form loss, friction, and other losses prescribed by the code user. This additional term is calculated by the equation

$$H_{loss} = 0.5 k_L v \quad (3\text{-}5)$$

where

k_L = loss coefficient corresponding with velocity v (unitless).

The loss coefficient k_L is related to the drag force calculated by Equation (3-1) as follows;

$$0.5 k_L \rho v^2 = F_p \Delta x \quad (3\text{-}6)$$

where

Δx = length of RELAP5 control volume for which flow losses are being calculated (m).

Solving the above equation for k_L, the result is

$$k_L = \frac{2(\Delta x)F_p}{\varepsilon \rho v^2} \quad (3\text{-}7)$$

The value of k_L as calculated above is used for calculating the flow losses in a porous medium such as the pebble bed of a PB-HTGR. An assessment of the model described above showed that the model represents the flow losses of gas flowing through a porous medium [19].

4. CONVECTIVE HEAT TRANSFER

While the convective heat transfer in BT-HTGRs is calculated with conventional heat transfer correlations, a convective heat transfer correlation for a porous medium was implemented to calculate the convective heat transfer in PB-HTGRs. The Tung correlation is used to calculate the convective heat transfer for forced flow [20, 21]. This correlation for the Nusselt number is

$$\mathrm{Nu}_{conv} = 0.29\mathrm{Re}^{0.8}\mathrm{Pr}^{0.5} \quad (4\text{-}1)$$

where

Nu_{conv} = Nusselt number for convection,

Re = Reynolds number,

Pr = Prandtl number.

The Nusselt number is related to the convective heat transfer coefficient by the equation

$$\mathrm{Nu}_{conv} = (\mathrm{hD}_p)/\mathrm{k} \quad (4\text{-}2)$$

where

h = convective heat transfer coefficient ($\mathrm{W/m^2 \cdot K}$),

D_p = diameter of pebbles (m),

k = thermal conductivity of gas (W/m·K).

The Reynolds number for the fluid in the interstices of the pebble bed is calculated by the equation

$$\mathrm{Re} = \rho\varepsilon|v|\mathrm{D}_p/\mu \quad (4\text{-}3)$$

where

ρ = density of gas ($\mathrm{kg/m^3}$),

ε = porosity of debris bed,

v = velocity of gas (m/s) (εv = superficial velocity),

D_p = diameter of pebbles (m),

μ = viscosity of gas (kg/m·s).

The Prandtl number for the fluid in the interstices of the pebble bed is calculated by the equation

$$\mathrm{Pr} = \mu c_p/k \quad (4\text{-}4)$$

where

μ = viscosity of gas (kg/ms),

c_p = heat capacity of gas (J/kg·K),

k = thermal conductivity of gas (W/m·K).

Equation (4-1) is based on experiments in which the Prandtl number ranged from 0.7 to 5, the Reynolds number ranged from 8 to 2400, and the bed porosity ranged from 0.4 to 0.5.

An alternative correlation to Equation (4-1) for calculating the Nusselt number for forced convection is the correlation presented by NO [10];

$$\mathrm{Nu}_{conv} = 1.27\mathrm{Pr}^{0.333}\ \mathrm{Re}^{0.36}/\varepsilon^{1.18} + 0.033\mathrm{Pr}^{0.5}\ \mathrm{Re}^{0.86}/\varepsilon^{1.07} \quad (4\text{-}5)$$

The porosity in the above equation is calculated by Equation (1-4).

The Nusselt number for natural convection is also calculated and compared with that calculated for forced flow. If the Nusselt number for natural convection is greater than that for forced convection, then the natural convection Nusselt number is applied. The natural convection Nusselt number is calculated by the equation [22]

$$\mathrm{Nu}_{nat} = \mathrm{KRa}^{0.25} \quad (4\text{-}6)$$

where

Nu_{nat} = Nusselt number for natural convection,

$$\mathrm{K} = \begin{cases} 0.3 & 0 \le \mathrm{Ra} < 50 \\ 0.4 & 50 \le \mathrm{Ra} < 200 \\ 0.5 & 200 \le \mathrm{Ra} < 10^6 \\ 0.6 & 10^6 \le \mathrm{Ra} \le 10^8 \end{cases}$$

Ra = Rayleigh number

The Rayleigh number in the above equation is calculated by the equation

$$\mathrm{Ra} = \mathrm{Gr} \bullet \mathrm{Pr} = \frac{\rho_g^2 g D_p^3 \beta \Delta T}{\mu_g^2}\mathrm{Pr} \quad (4\text{-}7)$$

where

g = acceleration of gravity ($\mathrm{m/s^2}$),

β = volume coefficient of expansion of gas (1/K),

ΔT = local temperature difference between pebbles and gas ($T - T_g$).

After the Nusselt number has been calculated , the volumetric rate of heat removal term in Equation (1-11) is then calculated by the equation

$$q_{cv}(r,z) = A_s Nu \frac{k}{D_h}(T - T_g) \qquad (4\text{-}8)$$

where

$q_{cv}(r,z)$ = heat transferred to gas by convection (W/m^3),

A_s = surface area per unit volume (m^2/m^3),

T = temperature of surface (K),

T_g = temperature of gas (K),

D_h = hydraulic diameter (D_p for PB-HTGR) (m).

The surface area of pebbles per unit volume is calculated on the basis that the pebbles are spherical in shape and uniform in size. The resulting equation is

$$A_s = \frac{6(1-\varepsilon)}{D_p} \qquad (4\text{-}9)$$

where

ε = porosity of debris.

For the BT-HTGR, A_s is equal to the surface area of the coolant channels per unit volume of block.

5. AIR INGRESS AND GRAPHITE OXIDATION

For long-term conduction cooldown accidents, air ingress and graphite oxidation may occur [23]. The ingress of air by molecular diffusion is modeled by applying Fick's First Law of Diffusion [17, 24]. If air diffuses from a break to the top of the reactor vessel, the distribution in fluid densities allows a natural circulation path to develop and the ingress of air is greatly accelerated [24]. The development of the natural circulation path is calculated by the conventional models in the SCDAP/RELAP5/ATHENA code [16]. The oxidation of graphite is divided into three regimes identified by temperature [25, 26, 27]. The rate of oxidation is subject to constraints due to mass transfer limits and the bulk flow rate of air. Air ingress and oxidation result in the gas in the reactor having various compositions of He, CO_2, CO, N_2, and A. The details of the SCDAP/RELAP5/ATHENA models for air ingress and graphite oxidation are described elsewhere [24].

6. EXAMPLE CALCULATION OF LONG-TERM COOLING OF HTGR.

An idealized problem was analyzed to test the heat transfer models developed for configurations and phenomena unique to a HTGR and to test the interface of these models with the previously developed and assessed models in SCDAP/RELAP5/ATHENA for calculating fluid behavior in reactor systems. A small block-type HTGR with structures containing flow paths for removal of post-shutdown decay heat by natural circulation of atmospheric air was analyzed. The idealized problem represents a conduction cooldown accident without ingress of air. The transient analysis began with the HTGR in a state corresponding with the end of the blowdown period following a large break in the coolant system. In this state, the reactor system was completely depressurized and no forced flow of cooling was occurring. The gas pressure in the reactor system throughout the analysis was equal to 0.1 MPa. The reactor core consisted of blocks of graphite with embedded fuel compacts (fuel rods) and holes for coolant flow. The outer radius of the fueled part of the reactor core was equal to 1.63 m and the outer region of the reflector region around the core was equal to 2.125 m. The height of the fueled part of the reactor core was equal to 2.98 m. The reflector regions below and above the fueled part of the core each had a height of 1.06 m. The reactor vessel had an inner radius of 3.82 m and a thickness of 0.1 m. The riser part of the system for the natural circulation of air was a series of 408 individual vertical channels arranged in a circle around the reactor vessel. The surfaces of the risers facing the reactor vessel were 2.5 m from the outer surface of the reactor vessel. The length of the risers (term $R_{uo} - R_{ui}$) in Figure 4) was equal to 0.254 m and the width of the risers (term W_u in Figure 4) was equal to 0.05 m. The risers had a wall thickness of 0.005 m. The spacing between the individual risers was equal to 0.05 m. The wall of the downcomer had an inner radius of 6.85 m and a thickness of 0.01 m. The inner radius of the containment was equal to 7.10 m. Air from the atmosphere flowed down through the space between the downcomer and the containment and flowed up through the series of individual risers. The containment had a thickness of 0.5 m and its outside surface was not in contact with earth. The inside surface of the containment had a steel liner with a thickness of 0.01 m.

The transient heat generation in the reactor core corresponded with the transient decay heat for scram of the reactor at a time of 0.0 s. At the start of the analysis and just after reactor scram, the total decay heat production in the reactor core was 1.76 MW and the power density in the fueled part of the reactor core was equal to 0.79×10^5 W/m^3. At 100,000 s, the power density was equal to 0.125×10^5 W/m^3. The heat generation was uniform in the axial and radial directions.

The five major components in the reactor system were each defined to have ten axial nodes. A schematic of the nodalization is shown in Figure 5. Each component had the same spacing and elevation of axial nodes. The core was defined to have 23 radial nodes. The number of radial nodes in the reactor vessel, risers, downcomer, and containment were 5, 8, 5, and 11, respectively. The coolant in the reactor vessel was defined to remain stagnant during the reactor transient. The upper ends of the downcomer and the risers were connected to

a control volume representing the atmosphere. The flow of the air through the downcomer and risers was modeled by two parallel stacks of control volumes with ten control volumes in each stack. A short horizontal control volume connected the bottoms of these two stacks of control volumes. The transient rate of flow of air by natural circulation through the downcomer and risers was calculated by SCDAP/RELAP5/ATHENA.

The transient behavior of the reactor was calculated from the beginning of complete depressurization (0.0 s) to 200,000 s (55.5 hours). The maximum temperature in the reactor core was calculated to increase to 1042 K at 77,700 s and then slowly decrease. For a similar conduction cooldown accident, BT-HTGRs with a larger reactor core than the relatively small reactor analyzed here are expected to have a greater maximum reactor core temperature. Figure 6 shows the maximum temperatures as a function of time of the reactor core, reactor vessel and containment. The maximum temperature of the reactor vessel did not exceed 600 K and changed slowly with time. The maximum temperature of the containment was 360 K. At 200,000 s, the effective thermal conductivities at various locations in the fueled part of the reactor core were calculated to range from 23 W/m·K to 26 W/m·K. At this same time, the effective thermal conductivities at various locations in the reflector region of the reactor core were calculated to range between 74 W/m·K and 80 W/m·K.

After about 150,000 s, natural circulation of air from the atmosphere removed most of the decay heat produced in the reactor core. Figure 7 shows the rate of heat production in the reactor core and the rate of heat removal by transfer to air circulating through the risers surrounding the reactor vessel. Figure 8 shows the transient velocity of the air in the risers at the mid-plane elevation. Natural circulation of air from the atmosphere was calculated to begin immediately after the start of the analysis. The velocity of the air in the risers ranged from 1.3 m/s to 1.6 m/s. The temperature of the atmospheric air was 304 K. Some heatup of the air occurred as it was flowing down the downcomer. The temperature of the air flowing out of the top of the risers ranged from 342 K to 350 K.

In summary, the SCDAP/RELAP5/ATHENA solution of the idealized test problem indicates that the new models added to the code are functioning properly and interfaced correctly with previously developed and assessed fluid behavior models. The code is prepared for more in-depth assessment and for preliminary evaluations of the performance of HTGRs.

7. CONCLUSIONS

Models have been implemented into the SCDAP/RELAP5/ATHENA code for the transient analyses of Pebble Bed and Block-Type High Temperature Gas Reactors (HTGRs). These models calculate aspects of behavior unique to HTGRs, including (1) transport of decay heat by conduction and radiation through porous and heterogeneous media to the exterior of a reactor core for the situation of a depressurized reactor coolant system with no forced coolant flow, (2) convective heat transfer and flow losses the porous medium of PB-HTGRs, (3) transport of decay heat by combination of radiation, natural convection and conduction from the exterior of a reactor core to ultimate heat sinks such as the atmosphere and earth surrounding the reactor building, (4) oxidation of graphite in the reactor core, and (5) ingress of air into the reactor core by molecular diffusion from a break in the reactor system. The SCDAP/RELAP5/ATHENA solution of an idealized test problem indicates that the new models added to the code are functioning properly and interfaced correctly with the previously developed and assessed fluid behavior models in the code. The code is prepared for an in-depth assessment of its capability for the transient analysis of HTGRs and provides an analysis tool for the preliminary evaluation of whether PB-HTGRs and BT-HTGRs can endure accidents without significant fission product release or other significant damage to the reactor system. The extended code also provides a system-wide analysis for interfacing with a Computational Fluid Dynamics (CFD) code to calculate complex flow distributions in certain regions of a PB-HTGR or BT-HTGR.

REFERENCES

[1]Gittus, J. H., 1999, "The ESKOM Pebble Bed Modular Reactor," Nuclear Energy, 38, No. 4, pp. 215-221.

[2] McNeill, C., 2001, "A PBMR in Exelon's future?", Nuclear News.

[3] Bennett, R., 2002, Nuclear News, pp. 33-34.

[4] DOE, 1994, "Evaluation of the Gas Turbine Modular Helium Reactor," DOE-GT-MHR-100002, Gas-Cooled Reactor Associates, San Diego, CA.

[5] Kunitomi, K. et al., 1998, "Conceptual Design of a 50-MW Severe-Accident-Free HTR and the Related Test Program of the HTTR," Nuclear Technology, Vol. 123.

[6] Rodriguez, C. and Baxter, A., 2001, "The Value of Helium-Cooled Reactor Technologies for Transmutation of Nuclear Waste," 9th International Conference on Nuclear Engineering, Nice, France.

[7] Nichols, D., 2001, "The Pebble Bed Modular Reactor," Nuclear News, pp. 24-40.

[8] Fletcher, C. D., 1988, *Computational Techniques for Fluid Dynamics,* Volume 1, Springer-Verlag, pp. 107-121.

[9] SCDAP/RELAP5-3D Code Development Team, 2001, "SCDAP/RELAP5-3D© Code Manual Vol. 2: Modeling of Reactor Core and Vessel During Severe Accidents," INEEL/EXT-02-00589.

[10] NO, H.C., 2001, "Description of PBR System Simulation Code," MIT.

[11] Tanaka, M. and Chisaka, F.,1991, "Effective Thermal Conductivities of Discontinuous and Continuous Solid Systems," Kagaku Kogaku Ronbunshu, 16, 1990, pp. 168-173, translated to English in Scripta Technica, Inc..

[12] SCDAP/RELAP5-3D Code Development Team, 2001, "SCDAP/RELAP5-3D© Code Manual Vol. 4: MATPRO – A

Library of Material Properties for Light-Water-Reactor Accident Analysis," INEEL/EXT-02-00589.

[13] Niessen, H. and Ball, S., 2000, H. Niessen and S. Ball, "Heat Transport and Afterheat Removal for Gas Cooled Reactors Under Accident Conditions," IAEA-TECDOC-1163, International Atomic Energy Agency.

[14] Davis, C.. 2003, Personal communication, Idaho National Engineering and Environmental Laboratory.

[15], Holman, J. P., 1981, *Heat Transfer*, McGraw-Hill Book Company, New York, New York.

[16] The RELAP5-3D Development Team, 2002, "RELAP5-3D Code Manual," INEEL-EXT-98-00834, Revision 2.0.

[17] Bird, R. B., Stewart, W. E., and Lightfoot, E. N., 1960, *Transport Phenomena*, John Wiley & Sons, New York, New York.

[18] Chung, M. and Catton, I. 1991, "Post-dryout heat transfer in a multi-dimensional porous bed, Nuclear Engineering and Design 128, pp. 289–304.

[19] SCDAP/RELAP5-3D Code Development Team, 2001, "SCDAP/RELAP5-3D© Code Manual Vol. 5: Assessment of Modeling of Reactor Core Behavior During Severe Accidents," INEEL/EXT-02-00589.

[20] Tung, V. X., 1988, "Hydrodynamic and Thermal Aspects of Two-Phase Flow Through Porous Media," Ph. D. Thesis, University of California, Los Angeles.

[21] Tung, V. X., and Dhir, V. K., 1993, "Convective Heat Transfer from a Sphere Embedded in Unheated Porous-Media," Journal of Heat Transfer, Transactions of the ASME, 115 (2), pp. 503-506.

[22] Edwards, D. K. and Denny, V. E., and Mills, A. Jr., 1979, *Transfer Processes*, McGraw-Hill Book Comp, New York, New York.

[23] Schaaf, T. Froehling, H., Hohn, H., and Struth, S., 1998, "The NACOK experimental facility for investigating an air ingress into the core of a high temperature reactor," Kerntechnik 63.

[24] Moore, R. L., 2001, Personal communication, Idaho National Engineering and Environmental Laboratory.

[25] Oh, C. and NO, H. C., 2003, "Development of Safety Analysis Codes and Experimental Validation for a Very-High-Temperature Gas-Cooled Reactor," International Nuclear Energy Research Initiative Project 2003-013-K.

[26] Oh, C., Merrill, B. J., Moore, R. L., and Petti, D. A., 2001, "Air Ingress Analysis on a High Temperature Gas-Cooled Reactor," ASME International Mechanical Engineering Congress and Exposition, New York, New York, November 11-16.

[27] Moormann, R., 1983, "Graphite Oxidation Phenomena during Massive Air Ingress Accidents in Nuclear High Temperature Gas Cooled Reactors with Pebble Bed Core," Ber. Bunsenges. Phys. Chem., 87, pp. 1086-1090.

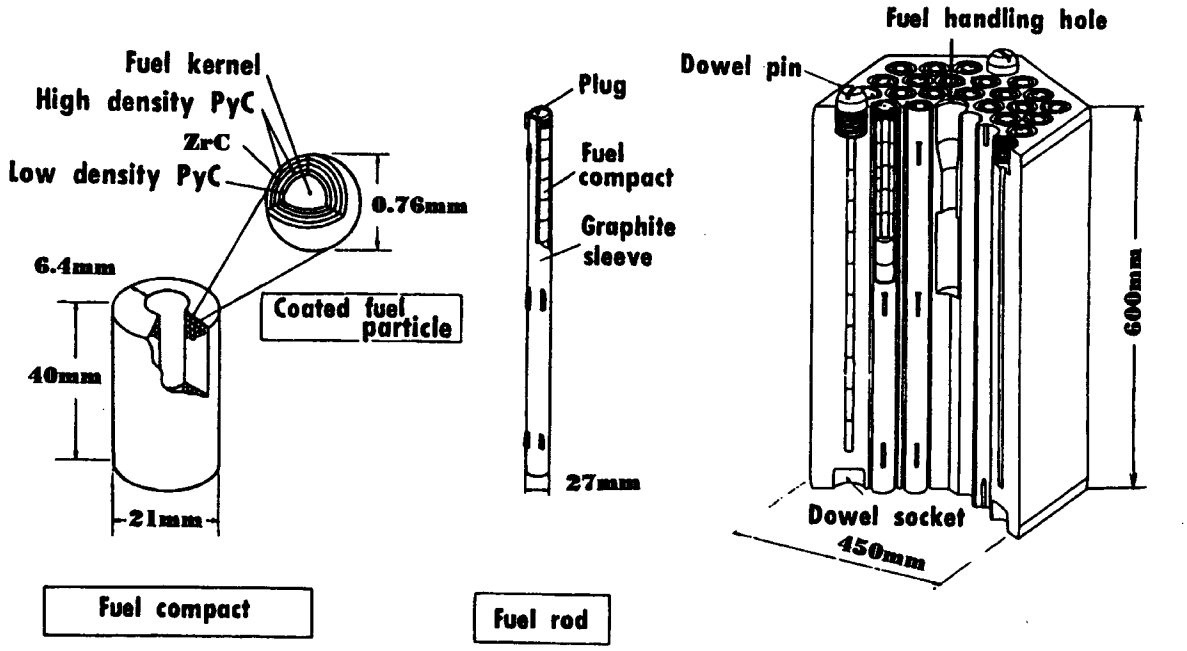

Figure 1. Example of configuration of fuel blocks in BT-HTGR.

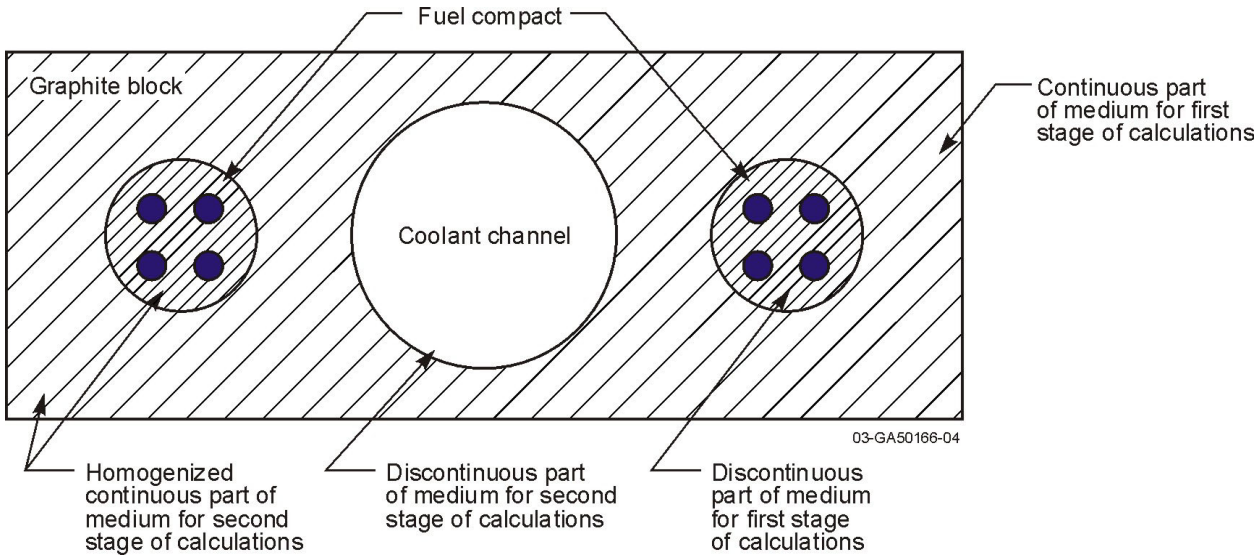

Figure 2. Schematic of calculation of effective thermal conductivity of homogenized fuel block

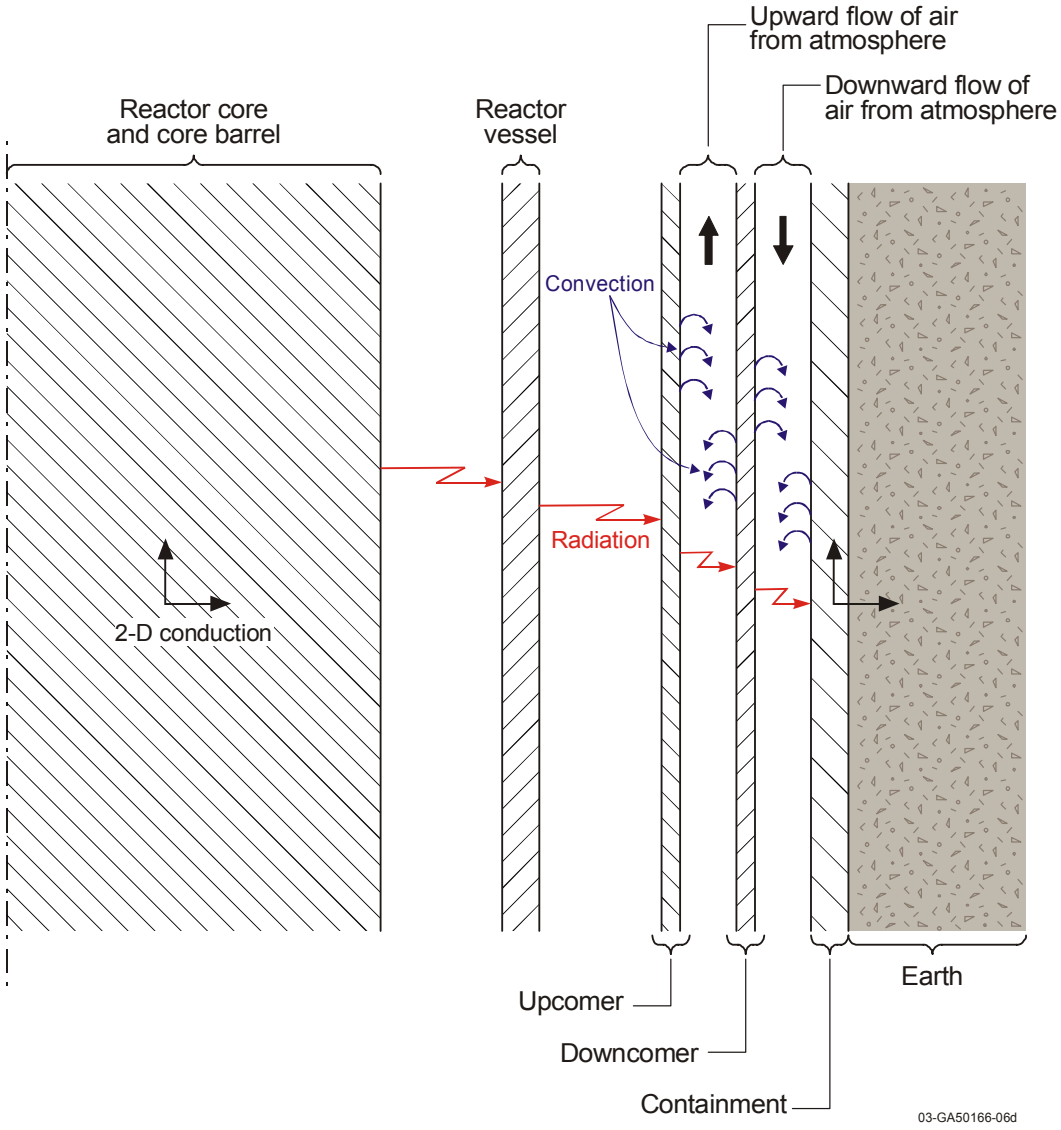

Figure 3. Schematic of modeling for passive cooling to atmosphere, containment, and earth.

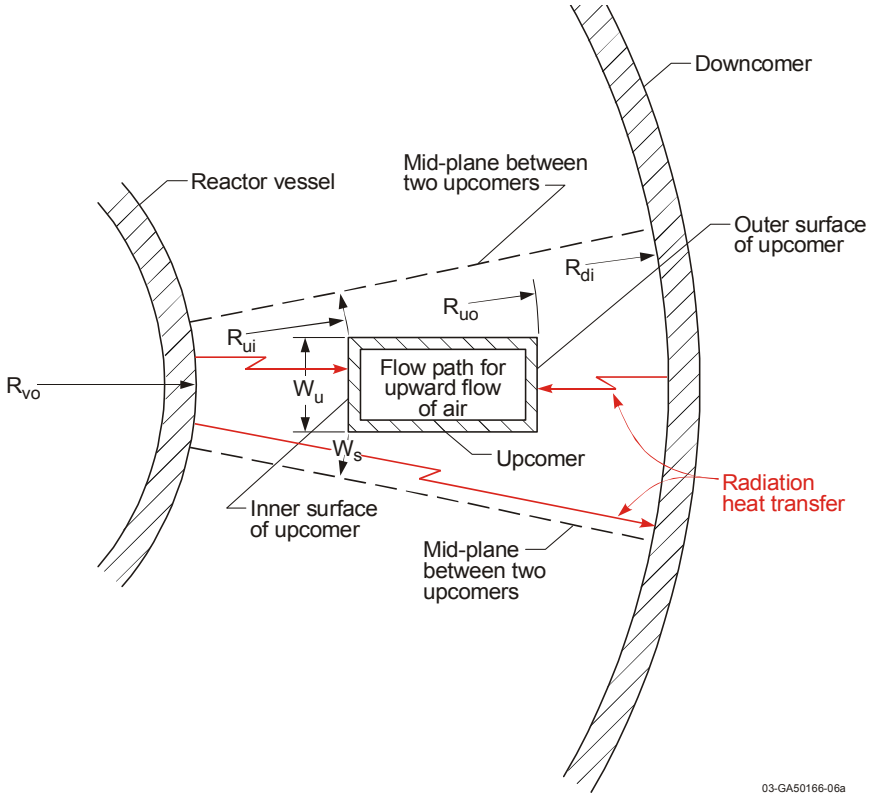

Figure 4. Radiation heat transfer for case of individual risers arranged in series around reactor vessel.

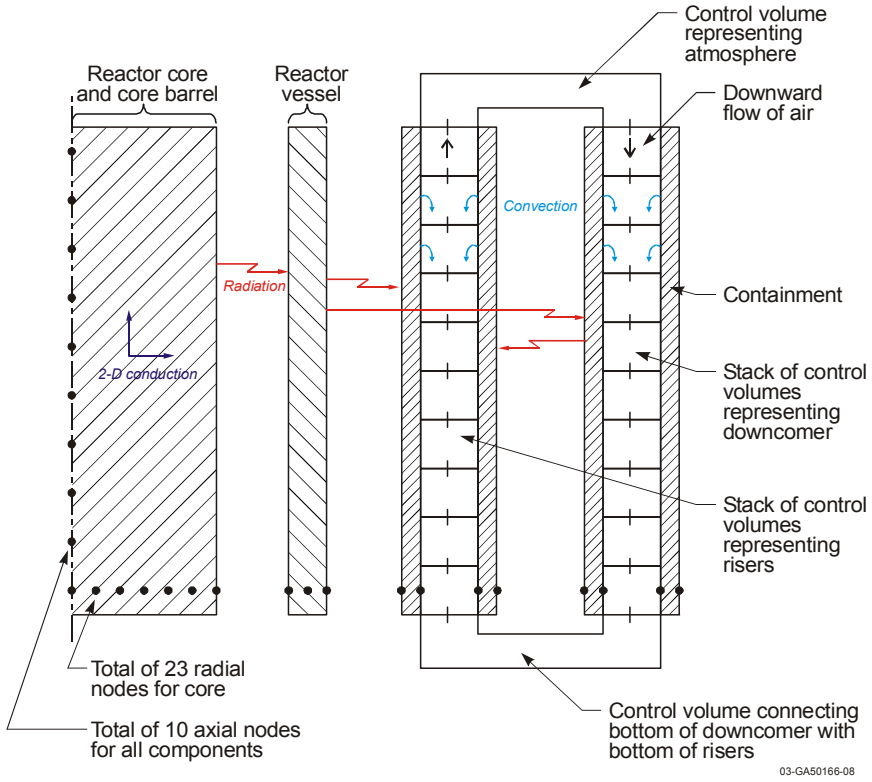

Figure 5. Schematic of nodalization for test problem involving transient analysis of Block-Type HTGR.

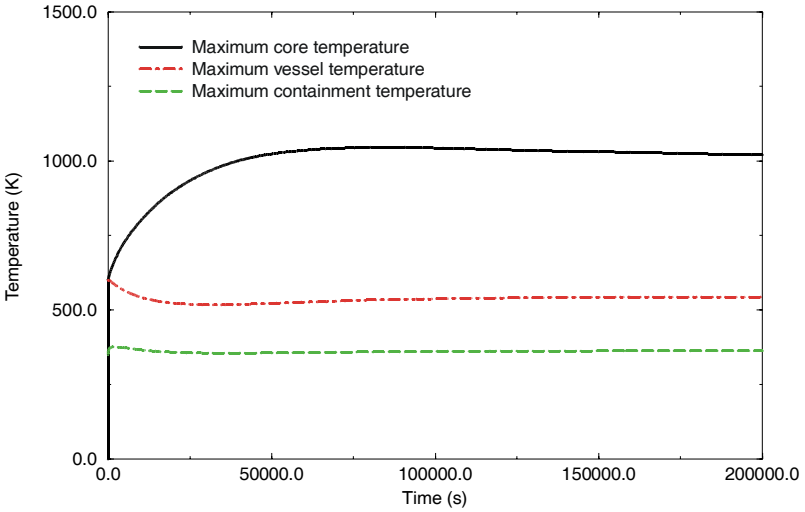

Figure 6. History of maximum temperatures in reactor core, vessel, and containment in analysis of Block-Type HTGR.

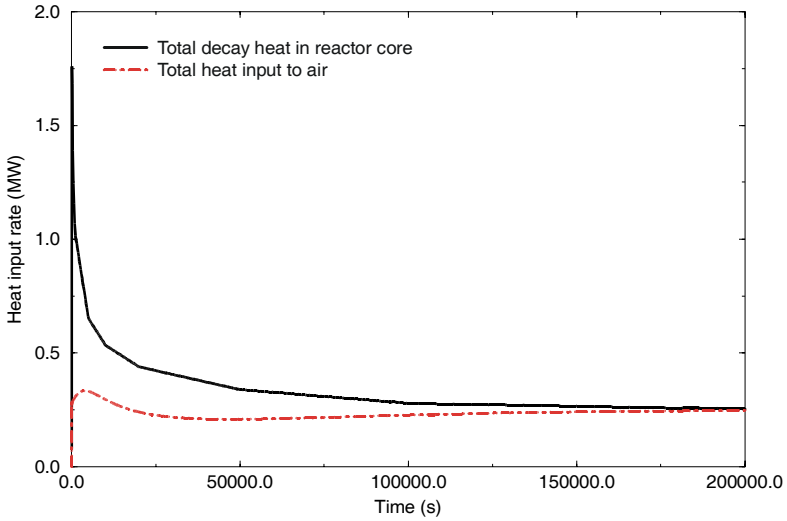

Figure 7. Comparison of rate of heat production in reactor core and rate of heat removal to air for Block-Type-HTGR.

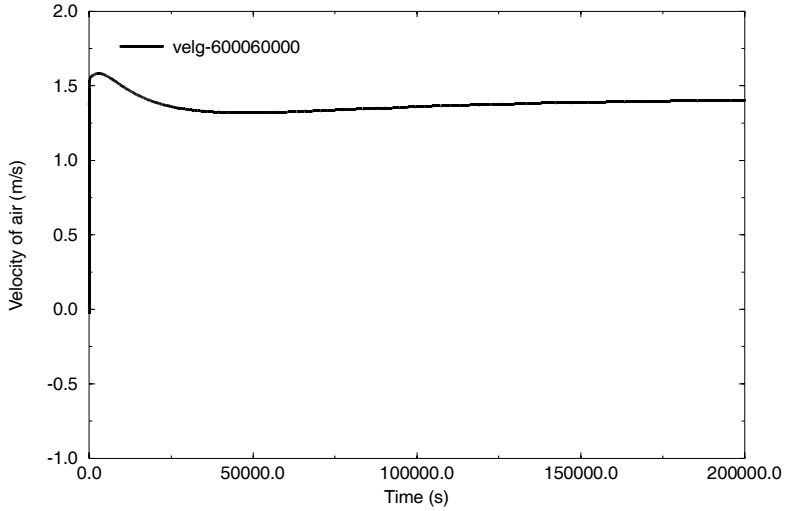

Figure 8. Velocity of air in risers at mid-plane elevation for Block-Type HTGR.